Ultrasound-Triggered Regulation of Blood Glucose Levels Using Injectable Nano-Network

Jin Di,
Joint Department of Biomedical Engineering, University of North Carolina at Chapel Hill and North Carolina State University, NC 27695, USA; Eshelman School of Pharmacy, Molecular Pharmaceutics Division, University of North Carolina at Chapel Hill, Chapel Hill, NC 27599, USA

Jennifer Price,
Joint Department of Biomedical Engineering, University of North Carolina at Chapel Hill and North Carolina State University, NC 27695, USA; Eshelman School of Pharmacy, Molecular Pharmaceutics Division, University of North Carolina at Chapel Hill, Chapel Hill, NC 27599, USA

Xiao Gu,
Department of Urology, Clinical Medical College at Yangzhou University, Yangzhou, Jiangsu 225001, P. R. China

Xiaoning Jiang,
Department of Mechanical Engineering, North Carolina State University, NC 27695, USA

Yun Jing*, and
Department of Mechanical Engineering, North Carolina State University, NC 27695, USA

Zhen Gu*
Joint Department of Biomedical Engineering, University of North Carolina at Chapel Hill and North Carolina State University, NC 27695, USA; Eshelman School of Pharmacy, Molecular Pharmaceutics Division, University of North Carolina at Chapel Hill, Chapel Hill, NC 27599, USA

Keywords

drug delivery; ultrasound; insulin delivery; diabetes; nano-network

Diabetes is a disorder of glucose regulation characterized by accumulation of glucose in the blood. It is a major public health problem currently affecting over 371 million people across the world, and this number is expected to grow to over 450 million by 2030.[1,2] The malfunction of glucose regulation arises from 1) insufficient secretion of insulin due to autoimmune-mediated destruction of pancreatic β-cells (type 1 diabetes) or 2) disorders of both insulin resistance and secretion (type 2 diabetes).[3] Current standard care for type 1 and advanced type 2 diabetic patients require consistent monitoring of blood glucose (BG) levels and subsequent insulin injections to achieve normoglycemia.[4] However, such

*zgu@email.unc.edu or zgu3@ncsu.edu; yjing2@ncsu.edu.

Supporting Information
Supporting Information is available online from Wiley InterScience or from the author.

traditional administration is often associated with pain, tenderness, microbial contamination, local tissue necrosis and nerve damage due to frequent subcutaneous insulin injections.[5]

In past decades, significant efforts have been made to overcome the limitation of conventional insulin delivery.[6,7] For example, long-term sustained insulin delivery, ranging from weeks to months using subcutaneously injected microcapsules or nanoparticles, can potentially enhance patient compliance and convenience.[8] However, such release behavior is passive in the absence of a pulsatile regulation controller. Lack of a tight control of BG levels is problematic and accounts for many chronic complications of diabetes such as limb amputation, blindness, kidney failure, and mental disorder. Closed-loop insulin release devices that are able to continuously and intelligently release insulin with response to BG levels changes hold great promise for improving quality of life of diabetic patients.[9,10] Currently, closed-loop electronic devices have been created by integration of a continuous glucose-monitoring sensor and an external insulin infusion pump.[11] Nevertheless, challenges, such as guaranteeing accurate glucose feedback and preventing failures in insulin infusions still exist.[12–14] A variety of synthetic approaches for glucose-mediated delivery of insulin have also been invented.[15,16] The majority of these systems have been limited to *in vitro* studies, due to difficulty in achieving fast response and pulsatile release profile *in vivo*. In this communication, we describe a spatiotemporally controlled insulin delivery system consisting of injectable polymeric nanoparticle-crosslinked network (designated nano-network (NN),[14] which can be noninvasively triggered by a focused ultrasound system (FUS). Using biodegradable poly(lactic-*co*-glycolic acid) (PLGA) as a matrix material, we have demonstrated that the resulting insulin encapsulated nano-network formulation activated by 30-sec FUS can effectively regulate blood glucose levels of type 1 diabetic mice in a long-term and pulsatile delivery manner.

Ultrasound has been shown to facilitate controlled drug delivery on demand, ranging in scope from releasing drugs in a degradable implant[17–19] to transdermal drug delivery.[20,21] Generally, the variation of release kinetics can be attributed to ultrasound-induced heating, acoustic streaming, or mechanical effects, such as nucleation, growth, and collapse of gas bubbles, a process referred to as inertial cavitation.[22–24] To date, a number of drug carriers have been explored to achieve ultrasound-responsive efficacy, including liposomes, micelles, microbubbles, and polymeric multilayered capsules.[25,26] Despite these, it remains elusive to demonstrate an ultrasound-assisted drug delivery system that would combine 1) sustained multiple activations over days, 2) ease of administration, and 3) biocompatibility without long-term side effect. A schematic of our formulation is displayed in Figure 1. Mixing and interacting of positively and negatively charged nanoparticles form a 3-dimentional (3D) cohesive gel-like nano-network *via* electrostatic forces. Such porous structure organized by colloidal particles at a nano scale have been reported to enable the release of payloads with near zero-order kinetics.[27,28] In addition, the noncovalently assembled nano-network has shear-thinning behavior due to the disruption of particle-particle interactions as the applied shear force increases. Once the external force is withdrawn, the strong cohesive property is recovered, which allows for convenient subcutaneous injection. We envision that dissociation of nano-network upon the trigger of ultrasound promotes the release of the “accumulated drug” stored in the unique porous

structure of the nano-network. FUS is specifically utilized to localize acoustic energy in the small injected area of nano-network for administration within a short period of time. As shown in Figure 1c, we expect that, like an insulin arsenal, the subcutaneously injected nano-network can maintain underneath the skin for a certain period and effectively release insulin for multiple times and regulate BG levels through a portable FUS.

We prepared insulin loaded nano-network by a double emulsion-based solvent evaporation method.[14] PLGA was selected as a matrix material due to its prominent biocompatibility and biodegradability.[29,30] To acquire oppositely charged nanoparticles, two natural polysaccharides, chitosan (positively charged)[31] and alginate (negatively charged)[32] were respectively applied as surfactants during the emulsion procedure to coat PLGA cores. The obtained nanoparticles had considerably charged coatings (zeta potential: 30.1 ± 1.9 mV for chitosan-coated nanoparticles (CS-NPs); −31.6 ± 2.3 mV for alginate-coated nanoparticles (AG-NPs)). Both CS-NPs and AG-NPs have high loading capacity of insulin and monodisperse particle sizes (Supporting information, Table S1). The average hydrodynamic particle sizes determined by dynamic light scattering (DLS) for CS-NPs and AG-NPs were 314 nm and 296 nm, respectively (Supporting information, Table S1, Figure S1). As demonstrated in Figure 2a, the cohesive nano-network was generated by mixing the oppositely charged nanoparticle solutions. The resulting nano-network displayed dramatically distinct viscosity behavior compared with pure nanoparticles (Supporting Information, Figure S2), indicating the formation of attractive electrostatic interaction and compact nanoparticle packing. The cohesive forces were reduced at high shear rate leading to the low viscosities that allows for facile injection of the nano-network through universal syringes (Figure 2b). The interaction of nanoparticles and formed porous structure with microchannels was observed by the scanning electron microscope (SEM) image in Figure 2c. To further illustrate the interaction between oppositely charged particles, insulin decorated with two different fluorescent dyes was encapsulated into CS-NPs and AG-NPs. The 3D laser scanning confocal microscopy (LSCM) indicated that the two particles in nano-network were tightly packed into agglomerates without noticeable mobility (Figure 2d).

To evaluate the efficacy of insulin release from the nano-network upon FUS activation, nano-network gels were collected in microcentrifuge tubes with 1×PBS solution. The sample microtubes were immobilized without FUS treatment for 10 min to determine initial basal insulin release from the insulin loaded nano-network. The focused ultrasound transducer (aperature diameter: 29.5 mm, focal length: 28 mm) operated at 950 kHz. The transducer was driven by signals generated by a function generator and amplified by an RF power amplifier. Three parameters of FUS that could affect drug delivery were varied in this study (Figure 3b–d): (a) the input voltage, (b) the pulse duration and (c) ultrasound administration time. The corresponding output power for each case was measured by an acoustic power radiation balance (Supporting Information, Table S2). The acoustic pressure was measured at the focal point by a needle hydrophone to determine the output waveform (Figure S3). In order to normalize the insulin release rate and to achieve favorable release condition, shortest FUS administration time combined with the most sustainable insulin release, the sample microtubes were submerged in a water bath in which the temperature was maintained at 37 °C, and fastened to a 3-axis stage sample holder, and positioned

precisely at the transducer focal point (Figure 3a). Figure 3b–d show that the release rate of insulin from nano-network was steadily increased when ramping up the input voltage or decreasing the pulse duration. Notably, the nano-network sensitively responded to the 30-sec treatment (input voltage: 400 mVpp, pulse duration: 20μs, output power: 4.31 W) and had an approximate 3.5-fold increase in the released insulin amount in a certain incubation period compared to the control sample with basal release (Figure 3d). The FUS-assisted enhancement can be attributed to a few factors that affect insulin diffusion from the network matrix, such as heating effect, acoustic streaming and cavitation. We applied a thermocouple probe to the test buffer for monitoring the temperature change immediately after the FUS treatment. There was no significant temperature increase (< 2 °C) recorded for the sample treated with FUS up to 4 min at the maximum input voltage (800 mVpp) and minimum pulse duration (20 μs). This is reasonable as the PBS solution has a low acoustic absorption coefficient.[33] To elucidate the importance of cavitation, control experiments were conducted in an exhaustively degassed buffer, where cavitation was minimized (Supporting Information, Figure S4). The insulin released amount in the degassed buffer was reduced by about 40%. We therefore conclude that cavitation induced by the ultrasonic waves is a major cause for the enhanced release profiles. We first assume that the dissociation of nano-network induced by shock waves created during inertial cavitation promotes rapid release of the insulin that “pre-released” and “stored” in the porous structures or microchannels of nano-network. Second, a rapid compression with subsequent expansion of the liquid induced by cavitation can also facilitate rupture of polymer chains of the particle matrix and thus trigger the release of insulin stored in the “aqueous nano-droplets” in the double emulsion formed particles. In addition to the action of shock waves, the collapse of cavitation bubbles could create pronounced perturbations in the surrounding liquid of nano-network. Therfore, we speculate that such a perturbation might increase the penetration of water species into the polymeric matrix, thereby promoting the following transport of insulin from cores of nanoparticles. Moreover, acoustic streaming could be responsible, which acts as a mild stirring force[34] causing the insulin release.

To demonstrate the pulsatile release profile triggered by FUS, we continuously performed multiple FUS treatment over time *via* optimized FUS conditions. As shown in Figure 3e, in every 20 min, FUS trigger was applied to the nano-network for 30 sec. Up to 8 prominent peaks of insulin release rate was recorded with the intermittent FUS triggers. Remarkably, a maximum of 80-fold increase in the insulin release rate was observed. The release rates associated with the FUS triggers were attenuated over time due to the depletion of the encapsulated insulin (Supporting Information, Figure S5). Interestingly, after multiple FUS triggers, the nano-network still stayed cohesive and there was no significant change in its viscosity behavior (Figure 3f). The compact packing and porous structure were also remained, characterized by SEM (Supporting Information, Figure S6). Moreover, the overall conformational structure of released insulin from nano-network *via* FUS was maintained, evaluated by its circular dichroism (CD) spectrum (Figure 3g).

We next assessed the *in vivo* efficacy of the insulin-loaded nano-network for ultrasound-triggered regulation of BG levels using STZ-induced adult diabetic mice. We hypothesized that the subcutaneously injected nano-network encapsulated with insulin could serve as an

insulin reservoir, the “valve” of which could be remotely opened by intermittent FUS and thereby regulate BG levels (Figure 4a). To substantiate this, the STZ-induced diabetic mice were divided into two groups and subcutaneously injected with PBS solution and insulin loaded nano-network gels (volume: 150 μL; insulin dose: 60 mg/kg) on the dorsal area, respectively. The blood glucose (BG) levels of administrated mice in each group were then monitored over time. As shown in Figure 4b, without FUS treatment, the passive release of insulin from nano-network effectively reduced BG levels over two weeks. However, the passive release was insufficient and two days after the “burst release” period, the BG levels became hyperglycemic (> 200 mg/dL). We then conducted FUS-triggered release experiments. As shown in Figure 4a. Anesthetized mice were immobilized on a plastic stage over a water bath. The nano-network injected skin area was shaved and immersed in water (37°C) through a slot in the stage. The focal point of the transducer was carefully adjusted to the position of the injection site, where a “bump” can be clearly identified. On the day 2 after subcutaneous injection (designated the day for injection as day 0), FUS was applied to the injection site of anesthetized mice for 30 sec and the BG levels of FUS-treated mice together with the control group injected with nano-network but without FUS treatment were subsequently recorded over time (Figure 4c). The FUS-trigger resulted in a significant decrease in BG levels. 10 min after trigger, the rapid decrease in BG level can be clearly detected. The BG level was declined into normoglycemia range (< 200 mg/dL) after one hour. The maximum change of BG level for mice treated with FUS was −159.5 ± 31.2 mg/dL (P<0.001, compared with the control group without FUS treatment). There was also a significant difference in the cumulative change in blood glucose (area under the curve, AUC) over 4 hours between the FUS-treated group and the control group. Correspondingly, significant increase of the plasma human insulin in mice treated with FUS was detected 30 min after trigger, in contrast to that of the control group, as shown in Figure 4d. Moreover, we performed the similar treatment on the day 4, day 7 and day 10. As shown in Figure 4c and Figure 4d, significant difference in the BG level and plasma insulin level changes due to the trigger of FUS was validated over time, indicating this method can be utilized for a long-term administration. Under the same FUS treatment conditions, the progressive decrease in the maximum reduced BG levels (Figure 4d) was likely due to the depletion of encapsulated insulin, which is consistent with the *in vitro* studies (Figure 3e). However, this could be potentially overcome by optimization of administration time as well as FUS power and pulse duration.

In a separate study, to achieve a pulsatile release profile *in vivo*, FUS-triggered treatment was intermittently conducted around every three hours on day 4. As demonstrated in Figure 4e, the hyperglycemic BG levels were effectively regulated into the normoglycemia range for up to three continuous cycles, using the same administration conditions. This pronounced release effect mediated by FUS further validates the feasibility of integration of the nano-network and portable FUS for a noninvasive approach to treating diabetes. Furthermore, the nano-network showed insignificant cytotoxicity and completely degraded after 4–6 weeks. The following histological examination (Supporting Information, Figure S7, S8) revealed no difference between the normal skin and the skin that has been interacted with the nano-network and exposed to ultrasonic irradiation as described above for multiple cycles (Figure 4c).

In summary, we have developed a novel means of ultrasound-triggered controlled drug delivery based on the use of an injectable nano-network. The gel-like 3D scaffold of nano-network can be effectively triggered to release insulin upon FUS-mediated administration. This system provides an unprecedented useful tool for noninvasive, rapid and pulsatile regulation of BG levels for diabetes treatment. It can also be extended to delivery of other drugs, therapeutic proteins or peptides in an intermittent and spatiotemporal release fashion. Furthermore, this method can be integrated with an ultrasound imaging system[35–37] for noninvasively monitoring degradation of the drug-contained formulation and facilitating the subsequent administration.

Experimental

Preparation of insulin loaded chitosan and alginate nanoparticles

Poly(lactic-*co*-glycolic acid) (PLGA) nanoparticles were prepared *via* a double emulsion method. Briefly, 4.8 mL organic phase (dichloromethane (DCM)) containing 180 mg PLGA (molecular weight: 40,000–75,000 kDa) was emulsified with 0.5 mL aqueous phase containing 30 mg human recombinant insulin (Invitrogen, USA) followed by sonication for 40 cycles (1 sec each with a duty cycle of 40%), and then the primary emulsion was immediately poured into 25 mL chitosan (Mn: 612 kDa; degree of deacetylation: 96.1 %) or alginate (Mv: 1.6×10^5) aqueous solution (1 %) and sonicated for 40 cycles. The double emulsion was subsequently transferred into 150 mL chitosan or alginate aqueous solution (0.1%). The mixed suspension was stirred at room temperature to eliminate DCM by evaporation. After 2 hours, the resulting nanoparticles were washed and collected by repeating a procedure of centrifuging at 10,000 rpm and suspending in deionized waster three times. In order to obtain the nano-network gels, the chitosan or alginate coated nanoparticles were separately dispersed in deionized water (w/v = 20%) and then mixed together (w/v = 1) in a bath sonicator for 2 min. The product was collected by centrifuging at 3000 rpm for 10 min and stored at 4 °C. The loading capacity (LC) and encapsulation efficiency (EE) of insulin encapsulated nanoparticles were determined by measuring the amount of non-encapsulated insulin through BCA (bicinchoninic acid) protein assay and using insulin-free particles as basic correction. LC and EE were calculated as: LC=(*A*-*B*)/*C*, EE=(*A*-*B*)/*A*, where *A* was expected encapsulated amount of insulin, *B* was the free amount of insulin in the collection solution and *C* was the total weight of particles (Supporting Information, Table S1).

In vitro release studies

To obtain the normalized insulin release amount, samples with 100 μL prepared nano-network and 400 μL PBS were tested at variations of input voltage (100 mVpp, 200 mVpp, 400 mVpp, and 800 mVpp), pluse duration (10 μs, 20 μs, 40 μs, 80 μs), and adiministration time (0.5 min, 1.0 min, 2.0 min and 4.0 min) at 37° C. At each predetermined point, the sample was centrifuged (5000 rpm, 30 sec) and 10 μL of the supernatant was removed for analysis. 10 μL of fresh PBS was then added to the tube to maintain a constant volume. Total insulin content was measured using a Coomassie Plus Protein Assay. The absorbance of the well was detected at 595 nm and the concentration was interpolated from an insulin standard curve.

In vivo studies using STZ-induced diabetic mice

The efficacy of the insulin-loaded nano-network for diabetes treatment was evaluated *in vivo* by assessment of glycemia in STZ-induced adult diabetic mice (male C57B6). All animals were treated in accordance with the Guide for Care and Use of Laboratory Animals, approved by the local committee. The BG levels of mice were continuously tested for two days before administration by collecting blood (~ 3 μL) from the tail vein and measuring using the Clarity GL2Plus Glucose Monitor (VWR, USA). Diabetic mice were randomly selected for each group administered with PBS solution, nano-network loaded with human recombinant insulin. 150 μL of the aqueous solution or nano-network was injected using a 1 cc syringe with a 19-gauge needle into the subcutaneous dorsum of mice (insulin dose: 60 mg/kg) post-anesthetization with 1 % isoflurane. The BG levels of each mouse was monitored over time (every 30 min or 2 hours for the first 12 hours in the day of administration and once per day in the morning for following days). For each FUS treatment (950 kHz; pulse duration: 20 μs; output power: 4.31 W; administration time: 30 sec), mice were shaved to expose the NN injection site, and then gently positioned on a home-made plastic platform with a slot in the center (Figure 4 (a)). BG levels were measured similarly over time after each treatment on the day 2, 4, 7 and 10 (Figure 4). To measure *in vivo* insulin concentration, blood samples (25 μL) were drawn from the tail vein of mice and collected into Sarstedt serum gel microtubes. Serum samples (5 μL) were stored frozen at −20 °C until assayed. Plasma insulin concentrations were determined using the human insulin ELISA kit (Calbiotech, USA).

Supplementary Material

Refer to Web version on PubMed Central for supplementary material.

Acknowledgments

This work was supported by the grant 550KR51307 from NC TraCS, NIH's Clinical and Translational Science Awards (CTSA, NIH) at UNC-CH and the NC State Faculty Research and Professional Development Award to Z.G..

References

1. Whiting DR, Guariguata L, Weil C, Shaw J. Diabetes Res. and Clin. Pr. 2011; 94:311.
2. Herman WH. Diabetes Care. 2013; 36:775. [PubMed: 23520368]
3. Owens DR, Zinman B, Bolli GB. Lancet. 2001; 358:739. [PubMed: 11551598]
4. Diabetes Care. 2013; 36:S11. [PubMed: 23264422]
5. N. Engl. J. Med. 1993; 329:977. [PubMed: 8366922]
6. Hinchcliffe M, Illum L. Adv.Drug Deliver. Rev. 1999; 35:199.
7. Stanley SA, Gagner JE, Damanpour S, Yoshida M, Dordick JS, Friedman JM. Science. 2012; 336:604. [PubMed: 22556257]
8. Renard E. Curr. Opin. Pharmacol. 2002; 2:708. [PubMed: 12482735]
9. Bratlie KM, York RL, Invernale MA, Langer R, Anderson DG. Adv. Healthcare Mater. 2012; 1:267.
10. Ravaine V, Ancla C, Catargi B. J. Control. Release. 2008; 132:2. [PubMed: 18782593]
11. Jankovec Z, Gruberova J, Krcma M, Rusavy Z. Diabetes Technol. The. 2013; 15:A42.

12. Fu Y, Kanderian S, Kshirsagar M, Kurisko D, Rebrin K, Steil GM. Diabetes Technol. The. 2013; 15:A79.
13. Khafagy ES, Morishita M, Onuki Y, Takayama K. Adv. Drug Deliver. Rev. 2007; 59:1521.
14. Gu Z, Aimetti AA, Wang Q, Dang TT, Zhang YL, Veiseh O, Cheng H, Langer RS, Anderson DG. ACS Nano. 2013; 7:4194. [PubMed: 23638642]
15. Brown LR, Edelman ER, FischelGhodsian F, Langer R. J. Pharmaceutical Sci. 1996; 85:1341.
16. Siegel RA, Gu YD, Lei M, Baldi A, Nuxoll EE, Ziaie B. J. Control. Release. 2010; 141:303. [PubMed: 20036310]
17. Kost J, Leong K, Langer R. Proc. Natl. Acad. Sci. 1989; 86:7663. [PubMed: 2813349]
18. Frinking PJA, Bouakaz A, de Jong N, Ten Cate FJ, Keating S. Ultrasonics. 1998; 36:709. [PubMed: 9651601]
19. Polat BE, Hart D, Langer R, Blankschtein D. J. Control. Release. 2011; 152:330. [PubMed: 21238514]
20. Prausnitz MR, Langer R. Nat. Biotechnol. 2008; 26:1261. [PubMed: 18997767]
21. Mitragotri S, Blankschtein D, Langer R. Science. 1995; 269:850. [PubMed: 7638603]
22. Ferrara KW. Adv. Drug Deliver. Rev. 2008; 60:1097.
23. Timko BP, Dvir T, Kohane DS. Adv. Mater. 2010; 22:4925. [PubMed: 20818618]
24. Kost J. Diabetes Technol Ther. 2002; 4:489. [PubMed: 12396743]
25. Tinkov S, Bekeredjian R, Winter G, Coester C. J. Pharm. Sci. 2009; 98:1935. [PubMed: 18979536]
26. Langer R. Accounts Chem. Res. 2000; 33:94.
27. Tao SL, Desai TA. Adv. Drug Deliver. Rev. 2003; 55:315.
28. Wang Q, Wang LM, Detamore MS, Berkland C. Adv.Mater. 2008; 20:236.
29. Anderson JM, Shive MS. Adv. Drug Deliver. Rev. 2012; 64:72.
30. Danhier F, Ansorena E, Silva JM, Coco R, Le Breton A, Preat V. J. Control. Release. 2012; 161:505. [PubMed: 22353619]
31. Kumar MNVR, Muzzarelli RAA, Muzzarelli C, Sashiwa H, Domb AJ. Chem. Rev. 2004; 104:6017. [PubMed: 15584695]
32. Pawar SN, Edgar KJ. Biomaterials. 2012; 33:3279. [PubMed: 22281421]
33. Vlad RM, Czarnota GJ, Giles A, Sherar MD, Hunt JW, Kolios MC. Phys. Med. Biol. 2005; 50:197. [PubMed: 15742939]
34. Sakharov DV, Hekkenberg RT, Rijken DC. Thromb. Res. 2000; 100:333. [PubMed: 11113277]
35. Niu DC, Wang X, Li YS, Zheng YY, Li FQ, Chen HR, Gu JL, Zhao WR, Shi JL. Adv. Mater. 2013; 25:2686. [PubMed: 23447424]
36. Nakatsuka MA, Mattrey RF, Esener SC, Cha JN, Goodwin AP. Adv. Mater. 2012; 24:6010. [PubMed: 22941789]
37. Yang F, Hu SL, Zhang Y, Cai XW, Huang Y, Wang F, Wen S, Teng GJ, Gu N. Adv. Mater. 2012; 24:5205. [PubMed: 22811026]

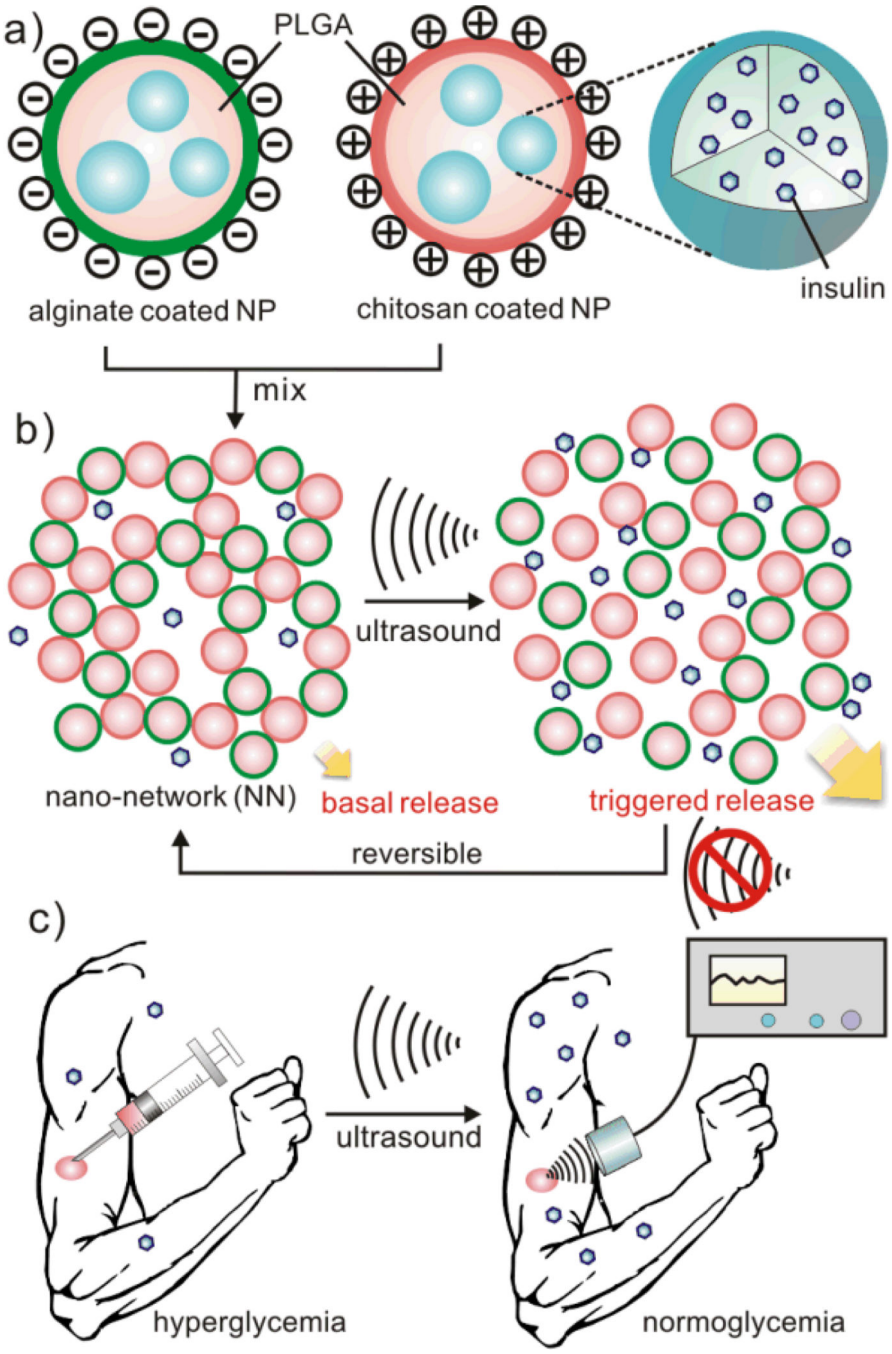

Figure 1. Schematic of the focused ultrasound (FUS)-mediated insulin delivery using nano-network

a) Nanoparticles (NPs) encapsulating insulin are made of PLGA and coated with chitosan and alginate, respectively. **b)** Nano-network (NN) is obtained by mixing oppositely charged nanoparticles together. The FUS triggers the dissociation of NN and promotes insulin release from the formulation. **c)** Schematic envision of noninvasive based long-term drug delivery triggered by the FUS after a subcutaneously injection of NN.

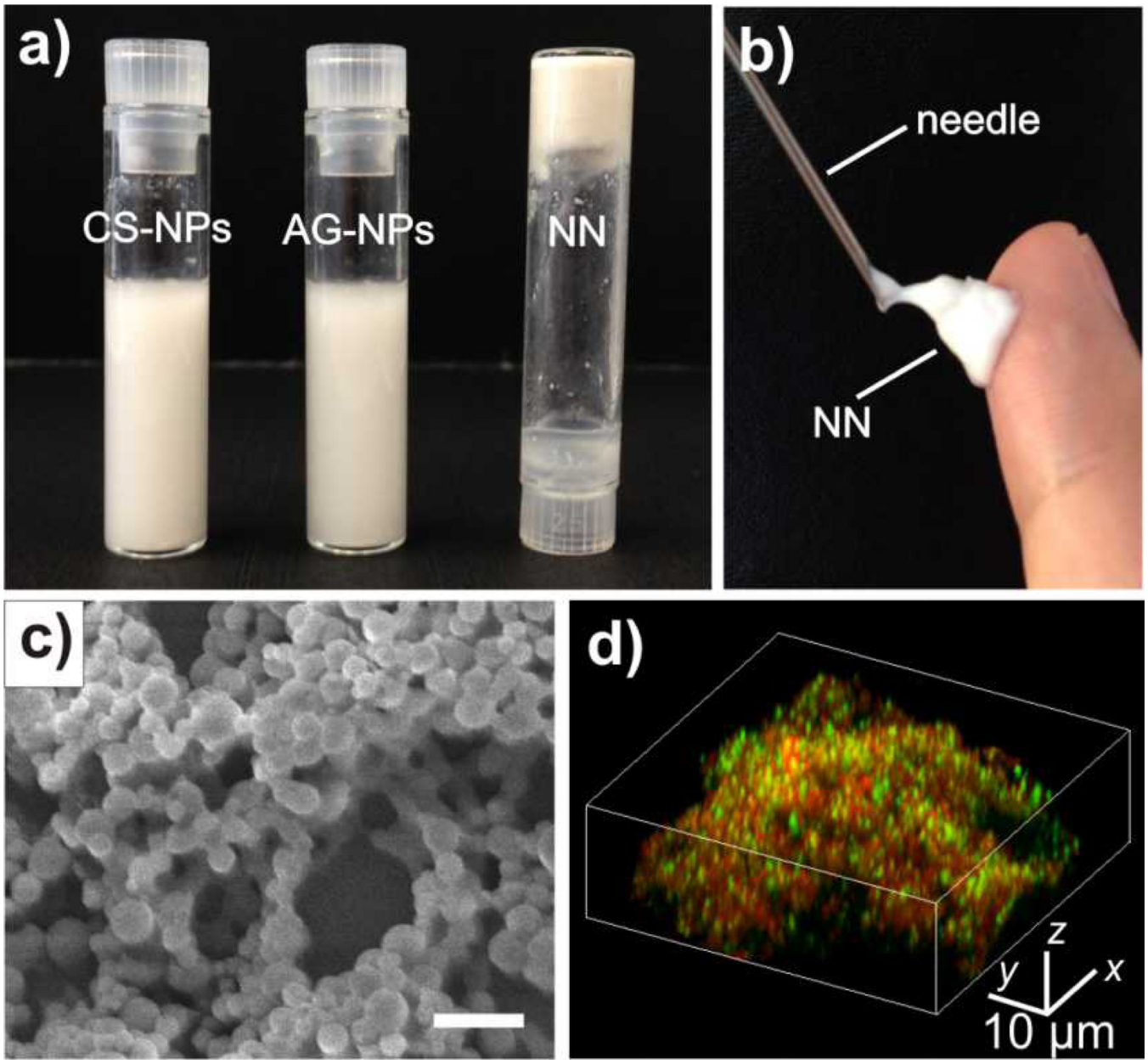

Figure 2. Characterization of the PLGA based nano-network encapsulating insulin

a) The adhesive PLGA NN was obtained by mixing well-dispersed chitosan NPs and alginate NPs together. **b)** The collected PLGA NN was injectable through a conventional syringe. **c)** The SEM image of formed nano-network with 3D porous structure. Scale bar: 1 μm. **d)** The laser scanning confocal microscopy image of the NN consisting of chitosan-coated NPs (encapsulated with FITC- stained insulin) and alginate-coated nanoparticles (encapsulated with rhodamine-stained insulin).

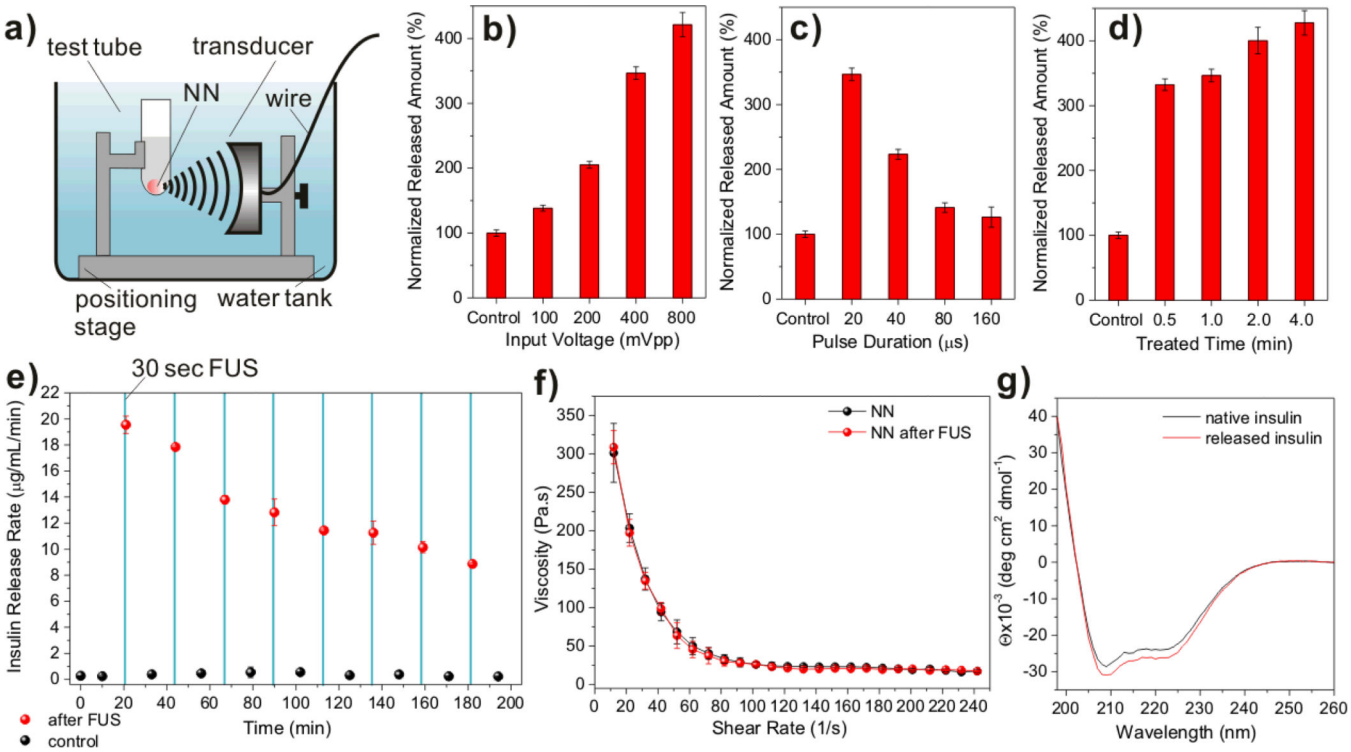

Figure 3. ***In vitro*** **insulin release of nano-network (NN) triggered by focused ultrasound (FUS)**

a) Schematic of the experimental apparatus. **b)–d)** Normalized insulin release rates upon variation of distinct ultrasound parameters in 1×PBS buffer at 37°C: vary input voltage at fixed time at 30 sec and pulse duration at 20 μs (b); vary pulse duration at fixed time at 30sec, input voltage at 400 mVpp (c); and vary administration time at fixed pulse duration at 20μs and input voltage at 400 mVpp (d). **e)** The pulsatile insulin release profile of the NN over time by the intermittent trigger of FUS in 1×PBS buffer at 37°C. The red spots indicate the release rate after the FUS treatment for 30 sec (950 kHz; input voltage: 400 mVpp; pulse duration: 20 μs; output power: 4.31 W); the black spots indicate the basal release rate. The blue solid columns indicate the FUS administration window. **f)** Viscosity and shear-thinning behaviors of the NN before and after FUS treatment. **g)** CD spectra of the native insulin solution and insulin released from the NN via FUS treatment at 37 °C. Data points in b)-f) represent mean ± SD (n = 3).

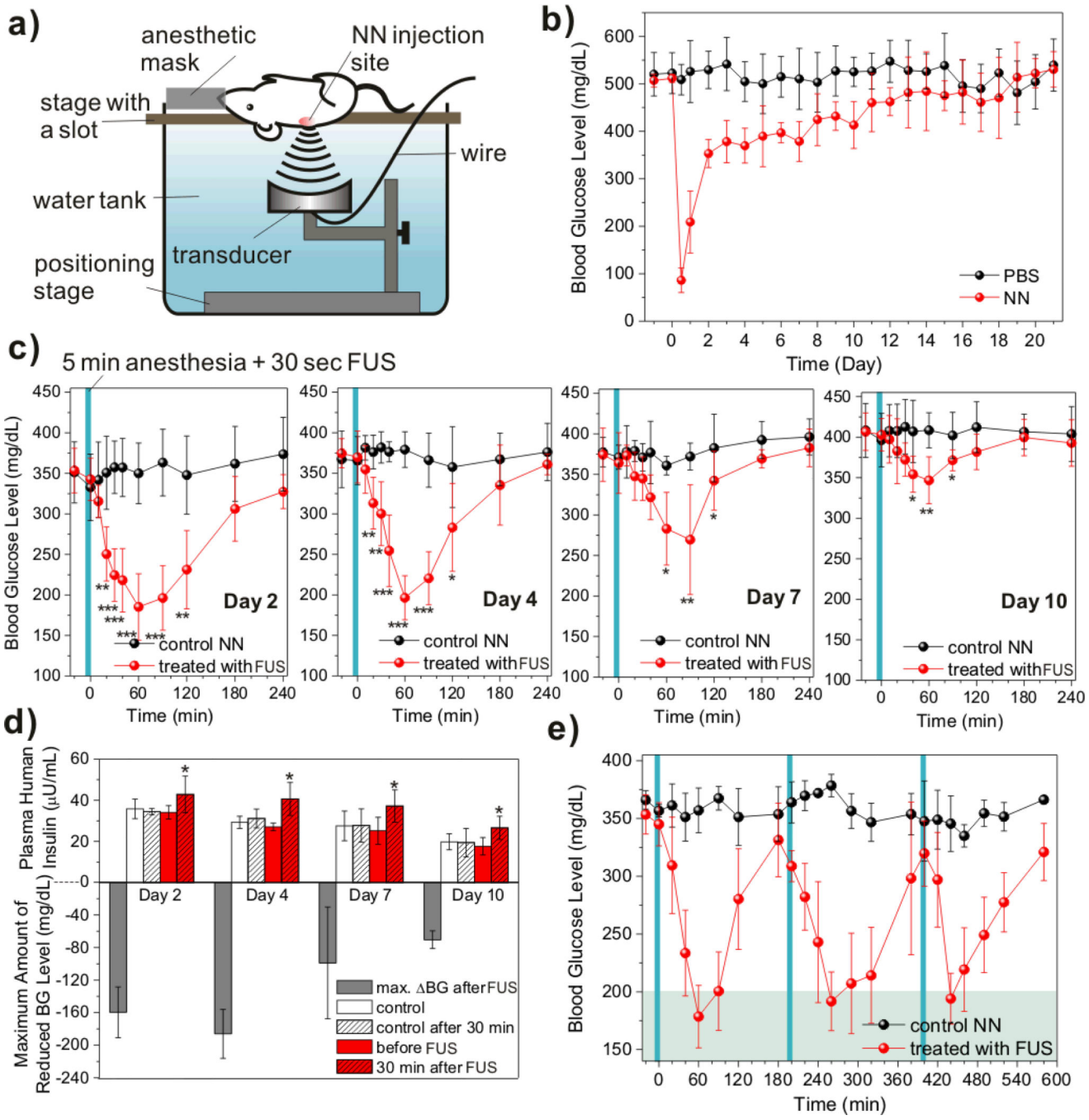

Figure 4. Focused ultrasound-mediated regulation of blood glucose levels *in vivo*

a) Schematic of the experimental apparatus. Anesthetized mice were immobilized on a stage over a water bath. The skin area for administration was immersed in water through a slot in the stage at the ultrasound focal point about 3 cm above transducer. **b)** Blood glucose levels in STZ-induced C57B6 diabetic mice (*n*=5) after subcutaneous injection with PBS or PLGA nano-network (NN) encapsulated with insulin. **c)** On the day 2, day 4, day 7 and day 10 after subcutaneous injection (designated the day for injection as day 0), FUS (950 kHz; input voltage: 400 mVpp; pulse duration: 20 μs; output power: 4.31 W) was applied to the

injection site on the anesthetized mice's dorsal area for 30 sec and the blood glucose levels of FUS-treated mice together with the control group injected with NN but without treatment were subsequently recorded over time. **d)** Plasma human insulin levels of mice before and 30 min after the FUS treatment on the day 2, day 4, day 7 and day 10. **e)** On the day 4, 3-cycle FUS treatment was applied and blood glucose levels were continuously recorded over time. The blue solid columns indicate the administration window, including 5 min anesthesia and 0.5 min FUS treatment. Asterisks indicate: **P*<0.05; ** *P*<0.01; ****P*<0.001 by Student's *t*-test. Error bars indicate ±SD.